

# Optimize Your Process



## Use Optimal Vacuum Solutions to Implement Renewable Energy

### Your added value

- Pumps for vacuum generation down to ultra-high vacuum
- Vacuum measurement and analysis equipment
- Leak detectors and integrity test systems
- Chambers, components and valves
- Pumping stations and customized solutions

# Electrodeposition as a Versatile Preparative Tool for Perovskite Photovoltaics: Aspects of Metallization and Selective Contacts/Active Layer Formation

Diego Di Girolamo\* and Danilo Dini\*

Perovskite-based photovoltaics (PV) is expected to play a central role in sustainable energy production during the next decades. Several companies are investing intensively to develop a market-ready product with efficiency and stability rapidly improving. The craft of making perovskite solar cells (PSCs) consists in the art of thin-film deposition, with electrodeposition (ED) representing one of the most versatile techniques available. The ED's role in the development of perovskite PV with its advantages, drawbacks, and perspectives is analyzed herein. The ED of inorganic or organic/polymeric selective contacts enables high-efficiency devices. Moreover, by exploiting properly designed functional barriers it is possible to rely on ED for the metallization of perovskite solar cells through the deposition of copper. The latter aspect could be particularly relevant for the development of silicon/perovskite tandem PV at the TW scale. On the other hand, the ED of the active layer is less successful to date mainly due to solubility issues of the perovskite in electrochemical polar solvents.

the need for vacuum as most printing/coating techniques. In contrast, ED allows a strict and direct control over nucleation and growth of the target film like gas phase-based techniques. As it will be discussed in the conclusive part of this perspective article (vide infra), ED is gaining momentum in the photovoltaics (PV) industry mainly due to the promising results on copper metallization with the primary intention of replacing the screen-printed silver busbars in silicon PV. However, in thin-film PV, the versatility of ED could be exploited much more intensively with respect to what is presently accomplished with ED in the ambit of PV. Perovskite PV is the emerging thin-film technology within PV and with regard to ED, the surface enclosing the potentialities of PV has been just scratched. In this perspective article, we will report a concise

description of the fundamental theory of ED in the initial section. In the successive section, the advancements concerning the ED of selective contacts will be reviewed including a discussion of the potentialities and limits of active layer electroplating. In the final section, the recent developments on metallization for perovskite solar cells (PSCs) via ED will be highlighted.

## 1. Introduction

In general terms, electrodeposition (ED) can be defined as the electrochemical technique that allows the deposition of thin films onto a conductive substrate the deposited film being a product of a redox reaction driven electrochemically. To a certain extent, ED could be considered a hybrid approach that shares most of the advantages of both chemical and physical thin-film deposition techniques. ED is conducted from precursor solutions without


## 2. ED for PV Purposes: General Features

Figure 1 shows the experimental electrochemical setup (an ordinary three-electrode cell) for the conduction of an ED process (sketch 1a), and the voltammogram (plot 1b) and the chronoamperogram (plot 1c) recorded with the apparatus of 1a when a hole-transporting layer of NiOOH is electrodeposited onto indium tin oxide (ITO).<sup>[1]</sup> This specific case is characterized by the presence of a nucleation loop in the voltammogram (Figure 1b), which is originated from the succession of the redox processes of oxidative electrodeposition of NiOOH and oxygen evolution reaction (OER) when the potential is scanned in the region of oxidative ED.

The loop is originated by the increasing electrochemical activity of the ITO substrate (working electrode (WE)) after the NiOOH is deposited on ITO. In the cathodic branch, the deposit of NiOOH is reduced to the Ni(II) hydroxide Ni(OH)<sub>2</sub>. With the appearance of the loop, cyclic voltammetry becomes a useful technique to identify the potential range within which ED takes place. The chronoamperogram starts with a low current value

D. Di Girolamo  
Department of Chemical, Materials and Production Engineering  
University of Naples "Federico II"  
80125 Naples, Italy  
E-mail: diego.digirolamo@unina.it

D. Dini  
Department of Chemistry  
University of Rome "La Sapienza"  
00185 Rome, Italy  
E-mail: danilo.dini@uniroma1.it

 The ORCID identification number(s) for the author(s) of this article can be found under <https://doi.org/10.1002/solr.202100993>.

© 2022 The Authors. Solar RRL published by Wiley-VCH GmbH. This is an open access article under the terms of the Creative Commons Attribution License, which permits use, distribution and reproduction in any medium, provided the original work is properly cited.

DOI: 10.1002/solr.202100993

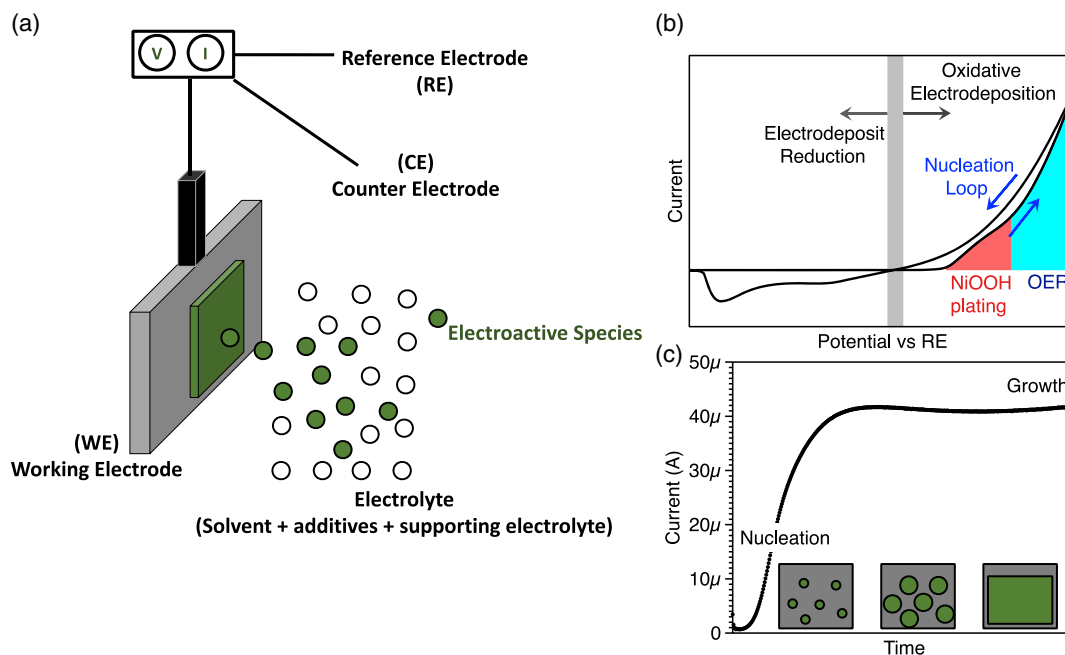


**Figure 1.** a) Schematic representation of the ED setup with a three-electrode electrochemical cell: working electrode (WE), counter electrode (CE), and reference electrode (RE). WE represents the ED substrate while CE assures the passage of the current through the electrolyte and warrants electrical continuity with the external circuit. RE allows the control of the potential of WE with respect to the constant potential value of RE (non-polarizable electrode). b) Typical cyclic voltammetry with the nucleation loop at high potential (regime of oxidative ED). c) Representative current transient recorded during the potentiostatic ED process of NiOOH on ITO (same system of Figure 1b).

due to the kinetic barrier for the nucleation of the electroactive NiOOH deposit. Afterward, the current increases due to the growth of the deposit as schematically reported in the inset of Figure 1c. The analysis of the current transient provides insights into the mechanism, kinetics, and dimensionality of ED as reported in.<sup>[1]</sup>

ED consists of the formation of a new adherent phase at the surface of WE through the occurrence of an electrochemical reaction conducted under potential/current control. In ED, the WE is then the substrate for the deposition of the film while the counter electrode (CE) serves to warrant the current flow through the circuit and is the site at which a second redox reaction occurs (the redox process at CE is not necessarily known or precisely defined). The employment of reference electrode (RE) allows the control of WE potential thanks to the fact that WE and RE are, respectively, polarizable and non-polarizable electrodes. The three electrodes setup (Figure 1a) allows a strict control over the current density ( $J$ ) – voltage ( $V$ ) relationships of the electrochemical system: the current flows between WE and CE and through the external circuit, while the voltage is continuously measured between the WE and RE. There exists various REs the Ag/AgCl being the most popular. CE is usually a metal (e.g., platinum) and there is not much interest into the details of the corresponding redox processes (vide supra), its only requirement being the ability to sustain the desired current. In contrast, the electrochemical reaction at the CE surface can affect the whole ED process in a twofold way: 1) the soluble products of the CE reaction alter the composition of the electrolyte and, consequently, the electrochemistry of the system (with variations of the electrical potential of redox reaction); and 2) the CE surface in contact with the electrolyte can alter its chemical

composition and morphology with time thus leading to a modification of the redox process at CE and its corresponding potential.

These considerations urge the operator to realize a clever design of the cell to achieve a reproducible and predictable ED process. The recovery of the side products of ED is another crucial aspect to reduce the costs and limit the environmental impact of this technique.

The characterization of the electrochemical properties of the deposits can be accomplished with the technique of cyclic voltammetry: it consists of the scan of WE potential versus the fixed potential value of a RE within a predefined range and at an adjustable rate. This allows the identification of the potential values at which the WE surface generates an electrochemical process. In Figure 1b, we show the typical cyclic voltammetry for Ni(AcO)<sub>2</sub> aqueous solution electrolyte with ITO as WE and Ag/AgCl as RE (CE: Pt wire). The cyclic voltammetry is conducted at a very slow scan rate (2 mV s<sup>-1</sup>) to minimize kinetic effects due to the slow diffusion of reactants, and to identify accurately the potential values at which electrochemical processes occur (for the details of the technique of cyclic voltammetry please refer to<sup>[2]</sup>). In this specific case, we observe a first voltammetric peak highlighted in red in the figure, which is attributed to the oxidation Ni<sup>2+</sup> → Ni<sup>3+</sup> with resulting precipitation/deposition of NiOOH. Upon potential increase, oxygen evolution reaction (OER) takes place and governs the electrochemistry of the system. When the potential scan is reversed a nucleation loop is observed (cathodic and anodic branches overlap), thus proving the modification of WE electrochemical activity. The presence of a nucleation loop is an indicator for the occurrence of deposition. The loop in the voltammogram usually arises for the faster kinetics of the

growth with respect to the nucleation process: the step of target film nucleation accelerates the reaction of deposition. In contrast, side reactions can complicate the quantitative analysis of the process of film deposition since the current density associated with the ORR is larger than that associated with the NiOOH electroplating with the loop originated by the faster oxidation of water on NiOOH (the growing target film) than on ITO (the substrate). In case the electrodeposited film is an electrical insulator, the electrochemical activity of the surface-modified WE will drastically decrease after the occurrence of the deposition.

In some cases, the cyclic voltammetry can be also considered as a potentiodynamic deposition route<sup>[3]</sup> for PV purposes and complements the other more common ED procedures of galvanostatic and potentiostatic deposition.<sup>[1,4]</sup> In galvanostatic deposition, the current density value between WE and CE is set at a predefined fixed value, while in the potentiostatic mode it is the voltage between WE and RE to be the fixed parameter. In both cases, if the values selected are suitable for the deposition, the film will grow with time and a chronopotentiogram (for the galvanostatic mode) or chronoamperogram (for the potentiostatic mode) will be recorded. Figure 1c shows the typical chronoamperogram for the system displaying the cyclic voltammetry of Figure 1b. The occurrence of a simple electron transfer reaction would have manifested itself with a  $J(t)$  profile presenting a time decreasing current until the reach of a steady-state value (kinetics under diffusion control in accordance to Cottrell equation<sup>[2,5,6]</sup>). It is observed, instead, an increase of the current density with time (Figure 1c) thus proving the enhancement of the electrochemical activity of the continuously modifying WE. At the onset of the applied potential, the reaction is slow (small current density) due to the kinetic barrier associated with the nucleation of the new phase. Successively the reaction accelerates with the growth of the deposited film until a steady state is reached. These kinds of transients are very insightful since provide an in situ monitoring of the electrochemical deposition. In this regard, several models<sup>[5–11]</sup> have been developed over the years to extract information such as the nucleation rate, the nuclei density, or the growth dimensionality. The application

of an appropriate model allows a precise and rational manipulation of the process without any additional complication to the instrumental setup with this representing one of the greatest advantages of ED over nonelectrochemical deposition techniques.

### 3. PSCs

PV based on metal halide perovskite as photoactive material is one of the most interesting technologies for the future of solar energy harvesting.<sup>[12]</sup> The unprecedented combination of high efficiency and ease of production, via low-cost printing techniques, promises a broad application ranging from tandem with silicon cells in MWh solar fields<sup>[13]</sup> to building-integrated photovoltaics<sup>[14]</sup> and solar-assisted electric transport, just to name a few. A PSC is based on a p-i-n junction (Figure 2), where the perovskite is the (pseudo)intrinsic layer that harvests the light and, consequently, creates pairs of free electrons and holes. The contacting n and p layers act selectively for collecting electrons and holes, respectively.

The p-i-n junction is sandwiched between two electrodes, which can be either transparent (ITO or fluorine-doped tin oxide (FTO)) or opaque (metals or carbon). The fabrication of PSCs consists of the sequential deposition of the various functional layers. On a lab scale, spin-coating is the prevailing technique for the deposition of each layer (except for the electrodes or specific materials such as C<sub>60</sub>, which is evaporated). However, spin coating has a limited attraction when considering industrial production for several reasons: it can't be implemented in sheet-to-sheet and roll-to-roll production lines and, most importantly, is not suitable for up-scaling. Therefore, it is not surprising that the record efficiencies of perovskite PV have been achieved with small area devices (less than 1 cm<sup>2</sup><sup>[15]</sup>). In contrast, ED is suitable for upscale and, in certain configurations, also for in-line production. In the following, we will discuss how ED of the perovskite layer has certain intrinsic limitations or difficulties, while the most interesting results have been achieved when looking at the ED of selective contacts and of substrate-electrodes.

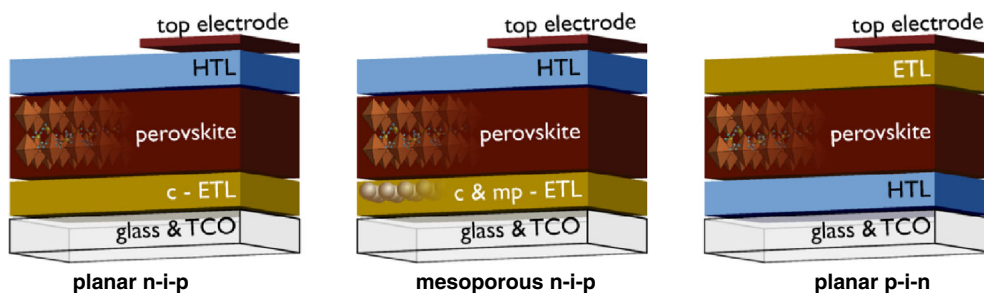


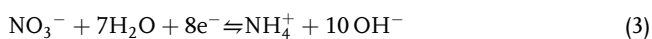
**Figure 2.** Various configurations of PSCs. Left sketch: The n-i-p configuration, also known as “direct architecture”, presents the n-type selective contact (electron-transporting layer, ETL) on the transparent substrate of the solar cell and can be either planar or mesoporous (middle sketch). The latter comprises a mesoporous layer of n-type metal oxide, such as TiO<sub>2</sub>. Right: the p-i-n or “inverted” architecture is characterized by the p-type selective contact coating the transparent substrate. The inverted configuration employs a commonly planar hole-transporting layer (HTL) and much less frequently a mesoporous one. Reproduced with permission.<sup>[12]</sup> Copyright 2013, American Chemical Society.

#### 4. Selective Contacts ED

Several transition metal oxides (TMOs) have been implemented as selective contacts in PSCs: TiO<sub>2</sub>,<sup>[16,17]</sup> NiO,<sup>[18,19]</sup> CuO,<sup>[20]</sup> V<sub>2</sub>O<sub>5</sub>.<sup>[21]</sup> When ED of TMOs from aqueous electrolytes is considered, the electrochemical generation of an oxy-hydroxide precursor phase at the WE represents the target.<sup>[22,23]</sup> The electrochemical reaction can involve a metal cation or the solvent with the process consisting of either a reduction at the cathode or an oxidation at the anode. In case of NiO, a p-type contact mainly implemented in the p-i-n architecture<sup>[24,25]</sup> (Figure 2) as HTL, it has been demonstrated that ED can be conducted both in anodic and cathodic modes. For such a reason of synthetic versatility, NiO represents a useful example for discussing the two different ED routes. In the anodic electrodeposition, the oxidation of Ni<sup>2+</sup> at the WE drives the nucleation and growth of the NiOOH phase onto the WE substrate. The overall reaction can be represented as follows



This two-step mechanism comprises the succession of an electrochemical (I) and a chemical (II) step for the formation of NiOOH precursor. The latter species, in turn, is transformed into NiO upon thermal annealing at 300 °C (final step of dehydration).<sup>[26,27]</sup> The authors conducted anodic ED from an aqueous solution of Ni(AcO)<sub>2</sub>. An interesting nanoflakes morphology in the NiO/NiOOH deposit was observed, which can be precisely tuned when the deposition is conducted potentiostatically when the potential value falls within the range 0.9–1.1 V versus Ag/AgCl (Figure 3a). Notably, the corresponding power conversion efficiency (PCE) of the NiO-based solar cells (Figure 3b) strongly correlates with the morphology of the resulting NiO film, especially for the direct influence morphology exerts on the parameter of the fill factor (FF, Figure 3c). Similar observations were reported by Park and coworkers<sup>[28]</sup> who exploited the cathodic ED of NiO. In this case, Ni(NO<sub>3</sub>)<sub>2</sub> is required as precursor [with Ni(II) as a starting reacting species] since the deposition proceeds through the following steps



Here, the electrochemical reaction involves the counteranion of the Ni(II) salt, i.e., nitrate (or alternatively the oxygen in the electrolyte) with the local increase of the pH acting as the driving agent of the precipitation of Ni(OH)<sub>2</sub>. The latter (vide supra) converts into NiO following the thermal annealing and dehydration.

Similar to our case, Park reported a higher efficiency for the more compact film, confirming the importance of controlling the morphology of the NiO layer. The high FF is attributable to excellent hole extraction benefiting from the nanoscale roughness of electrodeposited NiO. These results show that the control over the morphology of the hole selective contacts is important to increase the performances of PSCs.<sup>[26,28]</sup> The mechanisms going through the couples of steps (I)/(II) and (III)/(IV) can apply also for the deposition of other TMOs like TiO<sub>2</sub>,<sup>[29–31]</sup> ZnO,<sup>[32]</sup>

SnO<sub>2</sub>,<sup>[33,34]</sup> or CuO.<sup>[35]</sup> CuSCN, which is another suitable choice for a stable p-type interface<sup>[36]</sup> could be electrodeposited in a p-i-n configuration by reducing Cu<sup>2+</sup> in an SCN<sup>−</sup> containing electrolyte (mimicking the cathodic route for TMOs).<sup>[37]</sup>

As an alternative to metal oxides and other inorganic materials, various organic selective contact can be implemented into the PSCs as selective contacts. These include polymers<sup>[38]</sup> or “small-molecules.” The main advantages of organic materials are the possibility to alter the chemical structure and, consequently, to tune finely the energy levels and the chemical interaction with the perovskite surface.<sup>[39]</sup> The main drawback is the poor ability as a physical barrier for moisture, oxygen, or migrating ions within the device despite the possibility of intervening with the addition of nonpolar groups as substituents. Self-assembled monolayers appear as a promising solution to this problem, owing to their covalent bond with the transparent electrode.<sup>[40,41]</sup> Alternatively, extensive fluorination of the organic compounds improves the properties as a barrier for moisture.<sup>[42]</sup> The ED of organic polymers is usually referred to as electropolymerization.<sup>[43,44]</sup> A particularly interesting example is the work from Mei and coworkers, who demonstrated an efficiency above 20% exploiting an electropolymerized polyaniline (PAN) hole selective layer on FTO, in inverted architecture<sup>[45]</sup> (right sketch of Figure 2 and 3d–f). Electropolymerization of aniline proceeds during anodic polarization in presence of an acidic species. Mei employed dodecylbenzene sulfonic acid (DBSA) to conduct the anodic electropolymerization; however, it replaced the bulky organic anion with chloride to improve the properties as a substrate for the perovskite growth (Figure 3d). Benefiting from the improved conductivity of the Cl-PAN film with respect to DBS-PAN (Figure 3e) the efficiency of solar cells exceeded 20%, with respect to the literature reporting around 15% of PCE (Figure 3f). One of the advantages of electropolymerization is the low cost of reactants, since only the monomers are required when ED cell, solvents, and electrolytes are available. The aspect of reagents cost is in favor of the electrochemical preparation of conducting polymers from monomer electropolymerization versus the chemical route<sup>[46]</sup> since high purity polymers with a low polydispersity index are usually extremely expensive for the high costs of purification. Besides PAN, the electropolymerization of PEDOT on top of perovskite has been considered to show some limits in the performance of the resulting device.<sup>[47]</sup> A possible step further in the use of conductive polymers as selective contacts in perovskite PV could be moved by employing different types of poly- and oligo-thiophenes (especially the alkyl-substituted ones)<sup>[48–55]</sup> when this class of materials is deposited onto the substrate of interest via ED.<sup>[56,57]</sup> Besides the synthesis via electropolymerization, the class of polythiophenes (PTs) presents the additional advantage of being indifferently p-<sup>[58–61]</sup> and n-doped<sup>[62,63]</sup> via an electrochemical procedure of oxidation and reduction, respectively. This feature can lead to the preparation of electrochemically deposited and electrochemically doped hole-transporting layer HTL and electron-transporting layer (ETL) based on the same substrate of PT (or oligothiophene). Interestingly, oligothiophenes can undergo also phenomena of solid-state polymerization<sup>[64]</sup> due to the electrochemical coupling of these species (with typically 3–6 thiophenic units) when these are adsorbed and immobilized onto the substrate of interest. The phenomenon of oligothiophenes’ solid-state polymerization

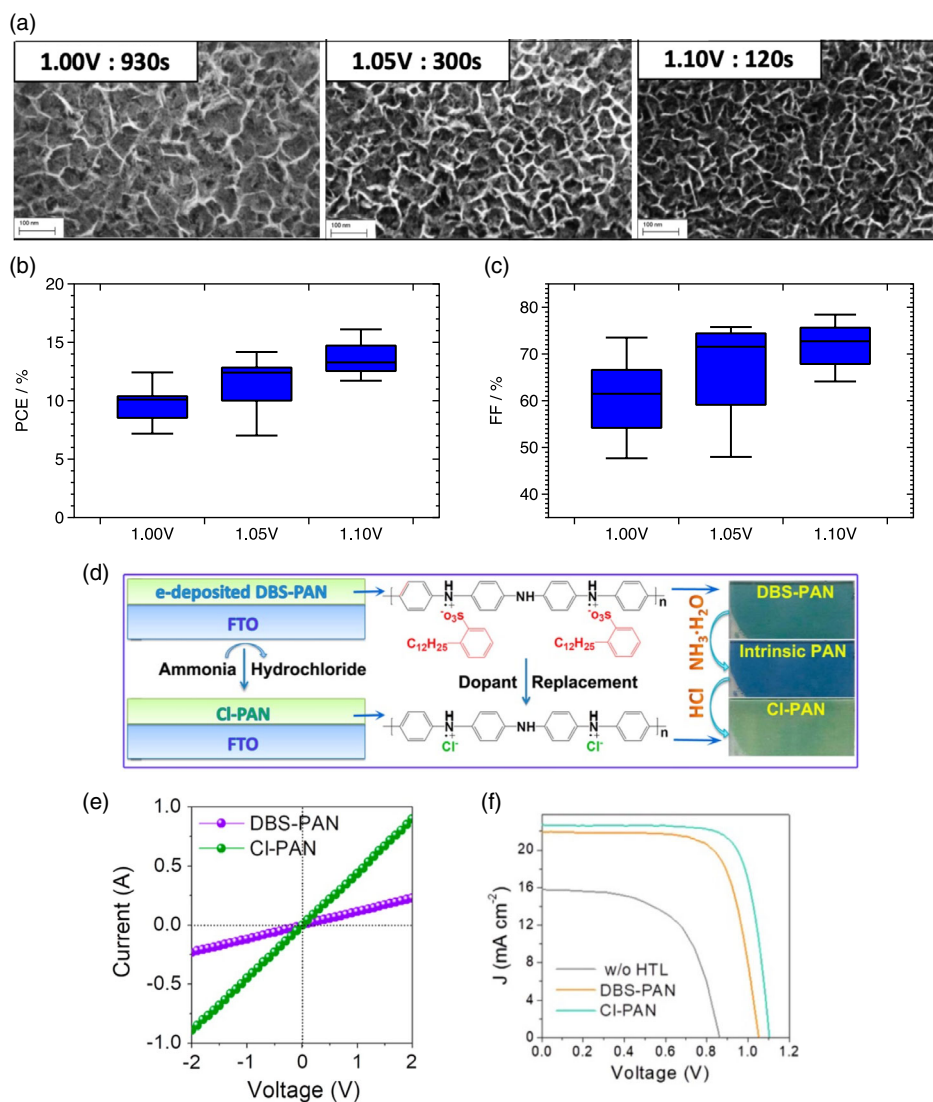


**Figure 3.** a) Morphology of NiO-HTL obtained from the thermal annealing of NiOOH after anodic potentiostatic ED. Porosity of the nanoflakes network is controlled through adjustment of deposition potential. Smaller pores and a more compact morphology is obtained at higher ED potentials (corresponding to faster ED). Reproduced with permission.<sup>[26]</sup> Copyright 2019, Elsevier B.V. b) PCE of inverted PSCs employing electrodeposited NiO at different potentials. PCE increases with the plating potential due to FF increase (c). d) Schematics of ED of polyaniline (PAN) and chemical conversion into the dodecyl benzenesulfonic acid (DBSA) doped DBS-PAN to obtain chloride doped polyaniline (Cl-PAN). Cl-PAN is obtained through an exchange reaction between the DBSA and HCl. e) The electrical conductivity of Cl-PAN results is larger than that of DBS-PAN with the consequent increase of the PCE of the PSCs due to larger  $J_{sc}$ ,  $V_{oc}$ , and FF (f). Reproduced with permission.<sup>[45]</sup> Copyright 2021, American Chemical Society.

could be profitably exploited in perovskite PV in case the operator wishes the polymerization of a limited number of adsorbed thiophenic units to attain films of selective contacts approaching the monolayer limit.

An important aspect that should be considered here is the effect of the TCO sheet resistance on the large area uniformity of the electrodeposited selective layer. With TCO substrates larger than a few cm<sup>2</sup>, an increasing voltage loss will be experienced moving away from the contacting area. The voltage drop will be larger for higher currents. Therefore, a possible strategy to minimize the non-uniformity of the film is to work with as low as possible current densities. However, this approach limits the versatility of the electrodeposition. A possible solution has been

proposed by De Rossi and coworkers,<sup>[65]</sup> who exploited a metallic grid to contact the TCO substrate for the electrodeposition. Notably, the grid could fit the dead-area of the p1-p2-p3 scribing employed to design Z-connected solar modules.<sup>[66]</sup>

## 5. Electrodeposited Perovskites

Undoubtedly, the most important and characteristic part of a PSC is the photoactive layer of halide perovskite itself. For that, it is fundamental to achieve a high quality of the perovskite in terms of crystallinity, phase purity, and morphology to minimize detrimental nonradiative recombination and push the efficiency

close to the Shockley–Queisser limit. In this respect, ED appears as an intrinsically problematic technique for the deposition of the perovskite film with all the reported desirable characteristics. The main reason for that is the not negligible solubility of perovskite in the polar solvents commonly used in electrochemistry. An important study has been reported by Samu and coworkers, who benchmarked the possibility to conduct electrochemical experiments on lead halide perovskites.<sup>[67]</sup> The only solvent that has been recognized to allow the conduction of electrochemical experiments on perovskites is dichloromethane ( $\text{CH}_2\text{Cl}_2$ ). This is a popular solvent in electrochemistry, but its use brings about serious concerns in terms of toxicity and safety. The latter two aspects are the priority when the industry has to consider the eventual adoption of electrochemical processes versus well-established, outperforming printing techniques, e.g., ink-jet printing or slot-die coating. Moreover, the solubility of the perovskite precursors in this solvent is quite limited (this is why  $\text{CH}_2\text{Cl}_2$  is compatible with perovskite) leaving small room for the design and the compositional variability of the electroplating solution.

Some interesting attempts to conduct part of the perovskite synthesis via an intermediate electrochemical step have been reported. In all cases, the perovskite synthesis is a multistep

process in which only one is electrochemical. Unlike the ED of TMOs, one of the perovskites presents the (important) difference that the different steps are conducted in different processes and environments and not at the same time. For the electrochemical preparation of perovskites, two different pathways can be outlined (Figure 4): it is possible to deposit lead oxide  $\text{PbO}_2$  (Figure 4a)<sup>[68,69]</sup> or  $\text{PbO}$ <sup>[70]</sup> similarly to what discussed in the case of transition metal oxides. The  $\text{PbO}_2$  film requires a  $\text{Pb}^{4+}$  reduction step, which can be carried out with  $\text{H}_2$ <sup>[71]</sup> or halohydric acids.<sup>[68,72]</sup> The  $\text{PbO}$  film is converted to  $\text{PbI}_2$  by acid leaching in hydroiodic acid (HI) solution and then submerged to a methylammonium iodide (MAI) solution to obtain the perovskite in the final state of utilization. Alternatively, the conversion steps from lead oxides to lead halide perovskites can be conducted in the gas phase,<sup>[72]</sup> as demonstrated on textured Si.<sup>[71]</sup>

This route can be simplified by the direct electrodeposition of  $\text{PbI}_2$ ,<sup>[73]</sup> by exploiting the reduction of  $\text{I}_2$  in a  $\text{Pb}^{2+}$  containing solution. However, the differences in solubility between  $\text{Pb}^{2+}$  and  $\text{I}_2$  make the electrolyte composition complicated with the additional requirement of an acid to stabilize it.  $\text{PbS}$  has been also considered as a precursor for perovskite ED.<sup>[74]</sup> Alternatively, metallic lead  $\text{Pb}$  can be cathodically electrodeposited

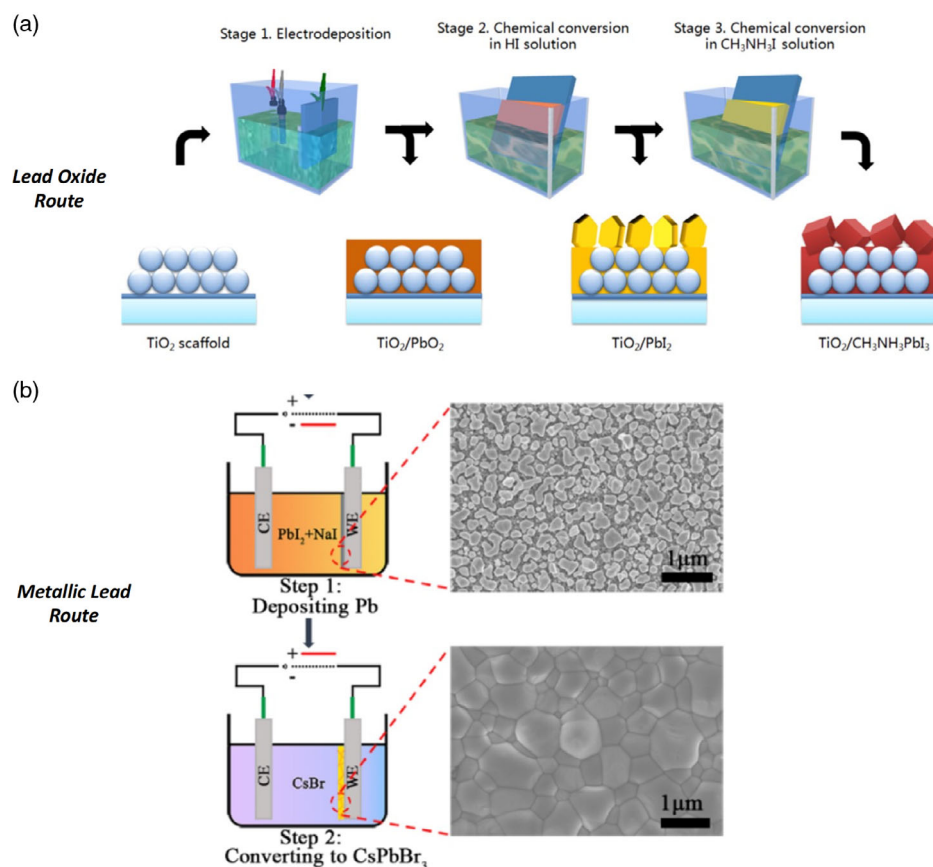


**Figure 4.** a) The lead oxide ( $\text{PbO}_2$ ) route for perovskite ED. Reproduced with permission.<sup>[69]</sup> Copyright 2015, Elsevier Ltd. In this process,  $\text{PbO}$  is electro-deposited on the conductive substrate of  $\text{TiO}_2$  as a precursor for lead iodide ( $\text{PbI}_2$ ). The latter is obtained by exposing the  $\text{PbO}$  layer to the hydroiodic aqueous solution. Finally, the perovskite is obtained by dipping the  $\text{PbI}_2$  film in a methylammonium iodide (MAI) solution. b) The metallic  $\text{Pb}$  route for perovskite ED:  $\text{Pb}$  is initially deposited on the conductive electrode via cathodic ED from a  $\text{Pb}^{2+}$  solution. After that,  $\text{Pb}$  is inserted in the perovskite structure ( $\text{CsPbBr}_3$  in this case) via dipping in a  $\text{CsBr}$  solution and the anodic polarization of the substrate to oxidize  $\text{Pb}$ . Reproduced with permission.<sup>[75]</sup> Copyright 2020, American Chemical Society.

from a  $\text{Pb}^{2+}$  solution.<sup>[75]</sup> Following that, the conversion to perovskite can occur in a single step by exposure to an acid solution containing the A-site cation and the halide. The main drawback of this procedure is the possibility to include unreacted metallic lead within the perovskite films with obvious adverse effects in terms of light absorption and shunt pathways into the device. In principle, the polyiodide melt route developed by Tarasov and coworkers<sup>[76]</sup> could be applied to electrodeposited lead films. This should minimize the amount of unreacted lead within the semiconducting layer. Another interesting study was conducted by Rakita and coworkers,<sup>[77]</sup> who evaluated the possibility to achieve lead-free tin perovskites by oxidizing Sn film with the obtainment of  $\text{CsSnI}_3$  and  $\text{MA}_2\text{SnI}_6$ . Despite the partial success in stabilizing the correct oxidation state of tin Sn(II), this result suggests that via electrochemistry it might be possible to control (and minimize) the amount of  $\text{Sn}^{4+}$  inside the tin perovskite films if the conversion of  $\text{SnI}_2$  to perovskite is conducted with an electrochemical setup and a cathodic polarization is applied.

## 6. Metallization

The metallic electrode of PSCs is of central relevance when considering the issue of long-term stability. The interaction between the metallic electrode and the perovskite film, through the selective contacts, has been soon identified as the common reason for device failure. For instance, thick carbon electrodes

in mesoporous triple stack PSCs have been exploited to pass the International Electrotechnical Commission (IEC) test the reverse bias stability,<sup>[78]</sup> important for the partial shadowing and, except for a few cases,<sup>[79]</sup> ignored so far. Gold (Au) electrodes have been observed to diffuse within the perovskite layer shunting the solar cells,<sup>[80]</sup> while photogenerated iodine from perovskite can react and decompose the metallic layer upon prolonged light exposure.<sup>[81]</sup> Wu and coworkers identified bismuth (Bi) as a stable metallic interlayer,<sup>[82]</sup> while others extended the lifetime of solar cells by introducing metal oxide nanoparticles<sup>[83]</sup> or sputtered ITO.<sup>[84]</sup> The latter method is particularly interesting and attractive since it is compatible with silicon/perovskite tandem PV, where a transparent electrode must be deposited on top of the perovskite wide gap cell.<sup>[85]</sup> The coupling of silicon and PSCs is considered one of the most useful applications of perovskite PV thanks to the mature industrial chain of silicon PV. However, such a coupling can bring about some concern in terms of material availability if the goal is the reach of the TW scale. Silver (Ag) is the top-performing metallic contact in PV but could represent an important issue toward the TW-scale. A recent analysis by Zhang and coworkers<sup>[86]</sup> estimated an upper limit well below 1 TW of the yearly production of PV if screen-printed Ag remains the electrode of choice for silicon (and therefore silicon/perovskite tandem) PV (Figure 5a).

To date, the best alternative to Ag is the electrodeposited copper (Cu) grid, which is approaching the ideal properties in terms of mechanical adhesion and conductivity required to avoid

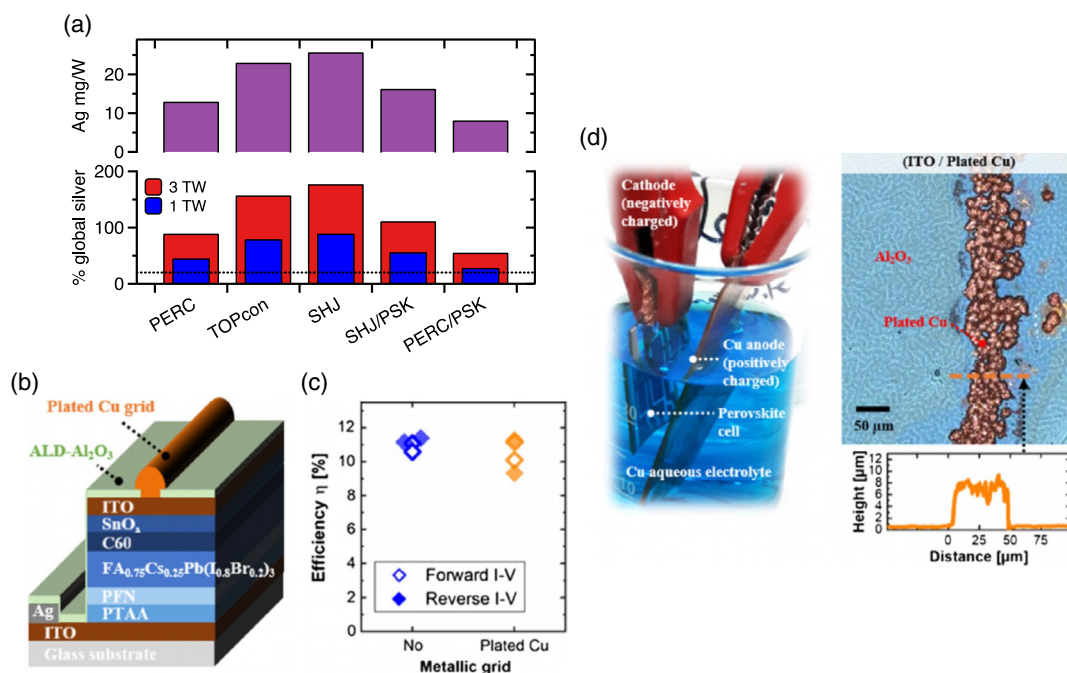


**Figure 5.** a) Ag consumption in mg/W for the relevant silicon PV technologies and derived silicon/perovskite tandem technologies (data extracted from table 3 of Ref [86]). In blue and red, the share of the total amount of Ag globally commercialized yearly to produce 1 and 3 TWp from the same silicon and silicon/perovskite PV technologies. The dashed line represents a share of 20%. It is possible to see that for most technologies the goal of 3 TWp per year is largely beyond the worldwide Ag availability, pointing to alternative metallization schemes for silicon and silicon/perovskite tandem PV. b) Architecture of PSCs with electro-deposited copper (Cu) grid as an alternative to Ag. c) By employing an atomic-layer-deposited  $\text{Al}_2\text{O}_3$  protecting layer, it is possible to electrodeposit Cu without PCE losses. Reproduced with permission.<sup>[87]</sup> Copyright 2021, Wiley-VCH. d) Picture of the solar cells submerged in the aqueous copper electrolyte for Cu plating and optical micrograph of Cu stripes with the profile. Reproduced under terms of the CC-BY license.<sup>[87]</sup> Copyright 2021, The Authors, Solar RRL published by Wiley-VCH GmbH.



optical or electrical losses. However, Cu electroplating on top of a PSC appears troublesome for the very same reason perovskite ED is difficult: perovskite is soluble in polar solvents and would not withstand the contact with the electrolyte. In this regard, it deserves to be highlighted the recent work by Hatt and coworkers,<sup>[87]</sup> who introduced an ultrathin atomic layer deposited Al<sub>2</sub>O<sub>3</sub> coating on top of a C60/SnO<sub>x</sub>/ITO triple stack electron selective layer (Figure 5b). Such a stratagem enabled the successful Cu electroplating on top of that, with negligible losses with respect to the control device (Figure 5c). This approach allowed to dip the perovskite devices in an aqueous electrolyte (Figure 5d) to deposit Cu lines with sizes compatible with that of the metallization schemes usually applied in silicon PV. Such a possibility brings the exploitation of perovskite PV closer to industrial feasibility.

## 7. Perspectives

The electrochemical synthesis of selective contacts appears to be the most relevant application of ED for perovskite PV. The strategies for the deposition of metal oxides and inorganic materials are well known with a few of them that have already demonstrated their effectiveness in perovskite PV. In this ambit, future efforts should be directed toward the attainment of deposits uniform over large areas (in the order of at least 1 m<sup>2</sup>). This aspect is affected by the resistivity of the transparent conducting oxides (TCOs), which act as substrates. Also, up-scaling to relevant size for industrial production needs to be demonstrated.

The use of conductive polymers should be considered more extensively in perovskite PV since these can be formed and doped electrochemically in situ onto a substrate of interest. This represents a good choice for the reduction of the costs of the chemical precursors and presents the additional advantage of tailoring the polymer properties in a more efficient way for the application of interest.

The attempts of electrodepositing materials on top of the perovskite or the perovskite itself are academically interesting but the poor stability of perovskite in common electrolytes<sup>[67]</sup> needs to be addressed more carefully before those procedures will gain a wider interest.

As far as the aspect of metallization is concerned, it is believed that the ED of the Cu grid is suitable for the mass-scale production of this technology, but further work in this direction is still necessary. The advancement in such a direction will have a tremendously important impact.

## Acknowledgements

D.D. acknowledges financial support from the University of Rome “La Sapienza” (Project ATENEO 2019, Prot. No. RM11916B756961CA) and from MIUR (Project PRIN 2017 with title “Novel Multilayered and Micro-Machined Electrode Nano-Architectures for Electrocatalytic Applications” - Prot. No. 2017YH9MRK).

Open access funding enabled and organized by Projekt DEAL.

## Conflict of Interest

The authors declare no conflict of interest.

## Keywords

electrochemistry, inorganic/organic HTL, nickel oxide, perovskite solar cells, polythiophene

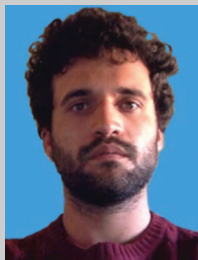
Received: November 23, 2021

Revised: January 13, 2022

Published online:

- [1] D. Di Girolamo, M. Piccinni, F. Matteocci, A. G. Marrani, R. Zanon, D. Dini, *Electrochim. Acta* **2019**, *319*, 175.
- [2] A. J. Bard, L. R. Faulkner, *Electrochemical Methods. Fundamental and Applications* JOHN WILEY & SONS; NEW YORK **2001**.
- [3] K. R. Prasad, N. Miura, *Appl. Phys. Lett.* **2004**, *85*, 4199.
- [4] K.-W. Nam, K.-B. Kim, *J. Electrochem. Soc.* **2002**, *149*, A346.
- [5] G. Gunawardena, G. Hills, I. Montenegro, B. Scharifker, *J. Electroanal. Chem.* **1982**, *138*, 225.
- [6] B. R. Scharifker, J. Mostany, *Encycl. Electrochem. and growth. Encyclopedia of Electrochemistry* **2007**.
- [7] P. Altimari, F. Pagnanelli, *Electrochim. Acta* **2016**, *206*, 116.
- [8] M. E. Hyde, R. G. Compton, *J. Electroanal. Chem.* **2003**, *549*, 1.
- [9] L. Heerman, A. Tarallo, *J. Electroanal. Chem.* **1999**, *470*, 70.
- [10] J. Mostany, J. Mozota, B. R. Scharifker, J. Mostany, *J. Electroanal. Chem. Interfacial Electrochem.* **1984**, *177*, 25.
- [11] M. Fleischmann, H. R. Thirsk, *Electrochim. Acta* **1959**, *1*, 146.
- [12] H. J. Snaith, *J. Phys. Chem. Lett.* **2013**, *4*, 3623.
- [13] J. Werner, B. Niesen, C. Ballif, *Adv. Mater. Interfaces* **2018**, *5*, 1700731.
- [14] M. Batmunkh, Y. L. Zhong, H. Zhao, *Adv. Mater.* **2020**, *32*, 2000631.
- [15] NREL Best Research-Cell Efficiencies, can be found under <https://www.nrel.gov/pv/cell-efficiency.html>, (accessed: February 2022).
- [16] A. Kojima, K. Teshima, Y. Shirai, T. Miyasaka, *J. Am. Chem. Soc.* **2009**, *131*, 6050.
- [17] W. S. Yang, B.-W. Park, E. H. Jung, N. J. Jeon, *Science* **2017**, *356*, 1376.
- [18] D. Di Girolamo, N. Phung, M. Jošt, A. Al-Ashouri, G. Chistiakova, J. Li, J. A. Márquez, T. Unold, L. Korte, S. Albrecht, A. Di Carlo, D. Dini, A. Abate, *Adv. Mater. Interfaces* **2019**, *6*, 1900789.
- [19] D. Di Girolamo, F. Matteocci, F. U. Kosasih, G. Chistiakova, W. Zuo, G. Divoitini, L. Korte, C. Ducati, A. Di Carlo, D. Dini, A. Abate, *Adv. Energy Mater.* **2019**, *9*, 1901642.
- [20] C. Zuo, L. Ding, *Small* **2015**, *11*, 5528.
- [21] H. Sun, X. Hou, Q. Wei, H. Liu, K. Yang, W. Wang, Q. An, Y. Rong, *Chem. Commun.* **2016**, *52*, 8099.
- [22] E. M. Garcia, V. F. C. Lins, T. Matencio, *Mod. Surf. Eng. Treat.* **2013**, chapter 5, 101, 122.
- [23] D. Tench, *J. Electrochem. Soc.* **1983**, *130*, 869.
- [24] D. Di Girolamo, F. Di Giacomo, F. Matteocci, A. G. Marrani, D. Dini, A. Abate, *Chem. Sci.* **2020**, *11*, 7746.
- [25] D. Di Girolamo, F. Matteocci, E. Lamanna, E. Calabrò, A. Di Carlo, D. Dini, in *AIP Conf. Proc.*, AIP Publishing LLC, Melville (NEW YORK) **2018**, p. 020011.
- [26] D. Di Girolamo, F. Matteocci, M. Piccinni, A. Di Carlo, D. Dini, *Sol. Energy Mater. Sol. Cells* **2020**, *205*, 110288.
- [27] M. Bonomo, D. Di Girolamo, M. Piccinni, D. P. Dowling, D. Dini, *Nanomaterials* **2020**, *10*, 167.
- [28] I. J. Park, G. Kang, M. A. Park, J. S. Kim, S. W. Seo, D. H. Kim, K. Zhu, T. Park, J. Y. Kim, *ChemSusChem* **2017**, *10*, 2660.
- [29] T.-S. Su, T.-Y. Hsieh, C.-Y. Hong, T.-C. Wei, *Sci. Rep.* **2015**, *5*, 16098.
- [30] S.-Y. Lin, T.-S. Su, T.-Y. Hsieh, P.-C. Lo, T.-C. Wei, *Adv. Energy Mater.* **2017**, *7*, 1700169.
- [31] K. S. Anuratha, H.-S. Peng, Y. Xiao, T.-S. Su, T.-C. Wei, J.-Y. Lin, *Electrochim. Acta* **2019**, *295*, 662.
- [32] A. Burgos, *Int. J. Electrochem. Sci.* **2018**, *13*, 6577.

- [33] J.-Y. Chen, C.-C. Chueh, Z. Zhu, W.-C. Chen, A. K. Y. Jen, *Sol. Energy Mater. Sol. Cells* **2017**, *164*, 47.
- [34] Y. Ko, Y. R. Kim, H. Jang, C. Lee, M. G. Kang, Y. Jun, *Nanoscale Res. Lett.* **2017**, *12*, 498.
- [35] X. Miao, S. Wang, W. Sun, Y. Zhu, C. Du, R. Ma, C. Wang, *Scr. Mater.* **2019**, *165*, 134.
- [36] N. Arora, M. I. Dar, A. Hinderhofer, N. Pellet, F. Schreiber, S. M. Zakeeruddin, M. Grätzel, *Science* **2017**, *358*, 768.
- [37] S. Ye, W. Sun, Y. Li, W. Yan, H. Peng, Z. Bian, Z. Liu, C. Huang, *Nano* **2015**, *15*, 3.
- [38] E. H. Jung, N. J. Jeon, E. Y. Park, C. S. Moon, T. J. Shin, T.-Y. Yang, J. H. Noh, J. Seo, *Nature* **2019**, *567*, 511.
- [39] M. Saliba, S. Orlandi, T. Matsui, S. Aghazada, M. Cavazzini, J. P. Correa-Baena, P. Gao, R. Scopelliti, E. Mosconi, K. H. Dahmen, F. De Angelis, A. Abate, A. Hagfeldt, G. Pozzi, M. Graetzel, M. K. Nazeeruddin, *Nat. Energy* **2016**, *1*, 1.
- [40] A. Magomedov, A. Al-Ashouri, E. Kasparavičius, S. Strazdaite, G. Niaura, M. Jošt, T. Malinauskas, S. Albrecht, V. Getautis, *Adv. Energy Mater.* **2018**, *8*, 1801892.
- [41] A. Al-Ashouri, A. Magomedov, M. Roß, M. Jošt, M. Talaikis, G. Chistiakova, T. Bertram, J. A. Márquez, E. Köhnen, E. Kasparavičius, S. Levenco, L. Gil-Escrig, C. J. Hages, R. Schlattmann, B. Rech, T. Malinauskas, T. Unold, C. A. Kaufmann, L. Korte, G. Niaura, V. Getautis, S. Albrecht, *Energy Environ. Sci.* **2019**, *12*, 3356.
- [42] Y. Kim, E. H. Jung, G. Kim, D. Kim, B. J. Kim, J. Seo, *Adv. Energy Mater.* **2018**, *8*, 1.
- [43] D. Dini, *Electrochem. Solid-State Lett.* **1999**, *1*, 217.
- [44] D. Dini, F. Decker, F. Andreani, E. Salattelli, P. Hapiot, *Polymer* **2000**, *41*, 6473.
- [45] Y. Mei, Z. Shen, S. Kundu, E. Dennis, S. Pang, F. Tan, G. Yue, Y. Gao, C. Dong, R. Liu, W. Zhang, M. I. Saidaminov, *Chem. Mater.* **2021**, *33*, 4679.
- [46] B. Scrosati, *Prog. Solid State Chem.* **1988**, *18*, 1.
- [47] G. F. Samu, R. A. Scheidt, G. Zaiats, P. V. Kamat, C. Janáky, *Chem. Mater.* **2018**, *30*, 4202.
- [48] C. Chang, H. Huang, H. Tsai, S. Lin, P. Liu, W. Chen, F. Hsu, W. Nie, Y. Chen, L. Wang, *Adv. Sci.* **2021**, *8*, 2002718.
- [49] S. Y. Ko, B. Nketia-Yawson, H. Ahn, J. W. Jo, M. J. Ko, *Int. J. Energy Res.* **2021**, *45*, 7998.
- [50] J.-Y. Lin, F.-C. Hsu, C.-Y. Chang, Y.-F. Chen, *J. Mater. Chem. C* **2021**, *9*, 5190.
- [51] W.-M. Gu, K.-J. Jiang, Y. Zhang, G.-H. Yu, C.-Y. Gao, X.-H. Fan, L.-M. Yang, *Chem. Eng. J.* **2022**, *430*, 133109.
- [52] S. Y. Ko, R. Singh, B. Nketia-Yawson, H. Ahn, J. W. Jo, J.-J. Lee, M. J. Ko, *Dye. Pigment.* **2021**, *190*, 109292.
- [53] B. Wang, L. Xue, S. Wang, Y. Li, L. Zang, H. Liu, Z. Zhang, Y. Li, *Appl. Phys. Lett.* **2021**, *119*, 133904.
- [54] C.-Y. Li, A. Chandel, J.-R. Wu, D. Thakur, S.-E. Chiang, K.-J. Cheng, S.-H. Chen, J.-L. Shen, S. H. Chang, *Sol. Energy Mater. Sol. Cells* **2021**, *237*, 111305.
- [55] J. Lim, M. Kim, W. Jang, J. K. Park, D. H. Wang, Versatile Pendant Polymer for Selective Charge Carrier Transport via Controlling the Supramolecular Self-Assembly. *ChemSusChem*, **2021**, *23*, pp. 5167–5178.
- [56] D. Dini, F. Decker, G. Zotti, G. Schiavon, S. Zecchin, F. Andreani, E. Salattelli, M. Lanzi, *Electrochim. Acta* **1999**, *44*, 1911.
- [57] L. Micaroni, D. Dini, F. Decker, M.-A. De Paoli, *J. Solid State Electrochem.* **1999**, *3*, 352.
- [58] M. Tsionsky, A. J. Bard, D. Dini, F. Decker, *Chem. Mater.* **1998**, *10*, 2120.
- [59] L. Micaroni, D. Dini, F. Decker, M.-A. De Paoli, *Electrochim. Acta* **1998**, *44*, 753.
- [60] D. Dini, F. Decker, G. Zotti, G. Schiavon, S. Zecchin, F. Andreani, E. Salattelli, *Chem. Mater.* **1999**, *11*, 3484.
- [61] D. Dini, E. Salattelli, J. Kankare, *J. Electrochem. Soc.* **2021**, *168*, 082507.
- [62] D. Dini, E. Salattelli, F. Decker, *Front. Chem.* **2021**, *9*, 1.
- [63] D. Dini, E. Salattelli, F. Decker, *J. Electrochem. Soc.* **2021**, *168*, 052506.
- [64] D. Dini, E. Salattelli, F. Decker, *J. Electrochem. Soc.* **2021**, *168*, 066521.
- [65] F. De Rossi, T. M. Brown, A. Reale, A. Di Carlo, *IEEE J. Photovoltaics* **2014**, *4*, 1552.
- [66] F. Di Giacomo, L. A. Castriotta, F. U. Kosasih, D. Di Girolamo, C. Ducati, A. Di Carlo, *Micromachines* **2020**, *11*, 1127.
- [67] G. F. Samu, R. A. Scheidt, P. V. Kamat, C. Janáky, *Chem. Mater.* **2018**, *30*, 561.
- [68] D. Ramírez, G. Riveros, P. Díaz, J. Verdugo, G. Núñez, S. Lizama, P. Lazo, E. A. Dalchiele, D. L. Gau, R. E. Marotti, J. A. Anta, L. Contreras-Bernal, A. Riquelme, J. Idigoras, *ChemElectroChem* **2020**, *7*, 3961.
- [69] H. Chen, Z. Wei, X. Zheng, S. Yang, *Nano Energy* **2015**, *15*, 216.
- [70] J. Huang, K. Jiang, X. Cui, Q. Zhang, M. Gao, M. Su, L. Yang, Y. Song, *Sci. Rep.* **2015**, *5*, 15889.
- [71] D. S. Lee, S. W. Seo, M.-A. Park, K. B. Cheon, S. G. Ji, I. J. Park, J. Y. Kim, *Electrochem. Commun.* **2019**, *103*, 120.
- [72] G. Popov, M. Mattinen, M. L. Kemell, M. Ritala, M. Leskelä, *ACS Omega* **2016**, *1*, 1296.
- [73] W. Li, J. Yang, Q. Jiang, R. Li, L. Zhao, *Sol. Energy* **2018**, *159*, 300.
- [74] S. Gozalzadeh, F. Nasirpour, S. Il Seok, *Chem. Eng. J.* **2021**, *411*, 128460.
- [75] X. Wang, S. Abbasi, D. Zhang, J. Wang, Y. Wang, Z. Cheng, H. Liu, W. Shen, *ACS Appl. Mater. Interfaces* **2020**, *12*, 50455.
- [76] I. Turkevych, S. Kazaoui, N. A. Belich, A. Y. Grishko, S. A. Fateev, A. A. Petrov, T. Urano, S. Aramaki, S. Kosar, M. Kondo, E. A. Goodilin, M. Graetzel, A. B. Tarasov, *Nat. Nanotechnol.* **2019**, *14*, 57.
- [77] Y. Rakita, S. Gupta, D. Cahen, G. Hodes, *Chem. Mater.* **2017**, *29*, 8620.
- [78] D. Bogachuk, K. Saddedine, D. Martineau, S. Narbey, A. Verma, P. Gebhardt, J. P. Herterich, N. Glissmann, S. Zouhair, J. Markert, I. E. Gould, M. D. McGehee, U. Würfel, A. Hinsch, L. Wagner, *Sol. RRL* **2021**, *2100527*, 2100527.
- [79] A. R. Bowering, L. Bertoluzzi, B. C. O'Regan, M. D. McGehee, *Adv. Energy Mater.* **2018**, *8*, 1702365.
- [80] S. Cacovich, L. Ciná, F. Matteocci, G. Divitini, P. A. Midgley, A. Di Carlo, C. Ducati, *Nanoscale* **2017**, *9*, 4700.
- [81] F. Fu, S. Pisoni, Q. Jeangros, J. Sastre-Pellicer, M. Kaweck, A. Paracchino, T. Moser, J. Werner, C. Andres, L. Duchêne, P. Fiala, M. Rawlence, S. Nicolay, C. Ballif, A. N. Tiwari, S. Buecheler, *Energy Environ. Sci.* **2019**, *12*, 3074.
- [82] S. Wu, R. Chen, S. Zhang, B. H. Babu, Y. Yue, H. Zhu, Z. Yang, C. Chen, W. Chen, Y. Huang, S. Fang, T. Liu, L. Han, W. Chen, *Nat. Commun.* **2019**, *10*, 1161.
- [83] M. Najafi, F. Di Giacomo, D. Zhang, S. Shanmugam, A. Senes, W. Verhees, A. Hadipour, Y. Galagan, T. Aernouts, S. Veenstra, R. Andriessen, *Small* **2018**, *14*, 1.
- [84] H.-Q. Wang, S. Wang, L. Chen, Z. Yin, S. Mei, Y. Zhong, Y. Yao, N. Li, J. Wang, W. Song, *Sol. Energy Mater. Sol. Cells* **2021**, *230*, 111278.
- [85] M. Jošt, E. Köhnen, A. B. Morales-Vilches, B. Lipovšek, K. Jäger, B. Maccò, S. Albrecht, Textured interfaces in monolithic perovskite/silicon tandem solar cells: advanced light management for improved efficiency and energy yield. *Energy & Environmental Science*, **2018**, *11*, pp. 3511–3523.
- [86] Y. Zhang, M. Kim, L. Wang, P. Verlinden, B. Hallam, *Energy Environ. Sci.* **2021**, *14*, 5587.
- [87] T. Hatt, Ö. Ş. Kabakli, P. S. C. Schulze, A. Richter, S. W. Glunz, M. Glatthaar, J. C. Goldschmidt, J. Bartsch, *Sol. RRL* **2021**, *5*, 2100381.



**Diego Di Girolamo** graduated in chemistry at the University of Rome La Sapienza, carrying out research on NiO as p-type selective contacts for lead halide perovskite solar cells. During his Ph.D., he worked on the electrodeposition of NiO on ITO to produce efficient inverted perovskite solar cells. His research interests include the degradation mechanisms of perovskites and, more recently, lead-free tin halide perovskite solar cells.



**Danilo Dini** obtained his Ph.D. in materials science in 1998 at University of Rome “La Sapienza,” with a thesis on the electrochemistry of conjugated polymers. During his postdoctoral time, he studied the electrochemiluminescence of organic materials (Fritz Haber Institut der Max Planck Gesellschaft, Berlin) and, successively, the nonlinear optical effects in macrocyclic complexes (University of Tübingen). He is currently at the Department of Chemistry of the University “La Sapienza” and is involved in solar energy conversion with the development of photoelectrochemical devices based on molecular sensitizers and nanostructured semiconducting electrodes. He has coauthored more than 150 papers.